X-ray powder diffraction

X-ray powder diffraction patterns of $[Co(Bz)(H_2O)_2)]Bz{\cdot}H_2O$ (**1**, *Bz* = benzoato) were measured on a RIGAKU D-Max/2500 diffractometer with rotating anode and RINT2000 vertical goniometer, in the range 2.5-40 º of 2θ using Cu $K\alpha_1$ radiation (λ = 1.5406 Å) and step 0.03 º; the theoretical powder diffraction pattern was calculated using the program PowderCell.[1]

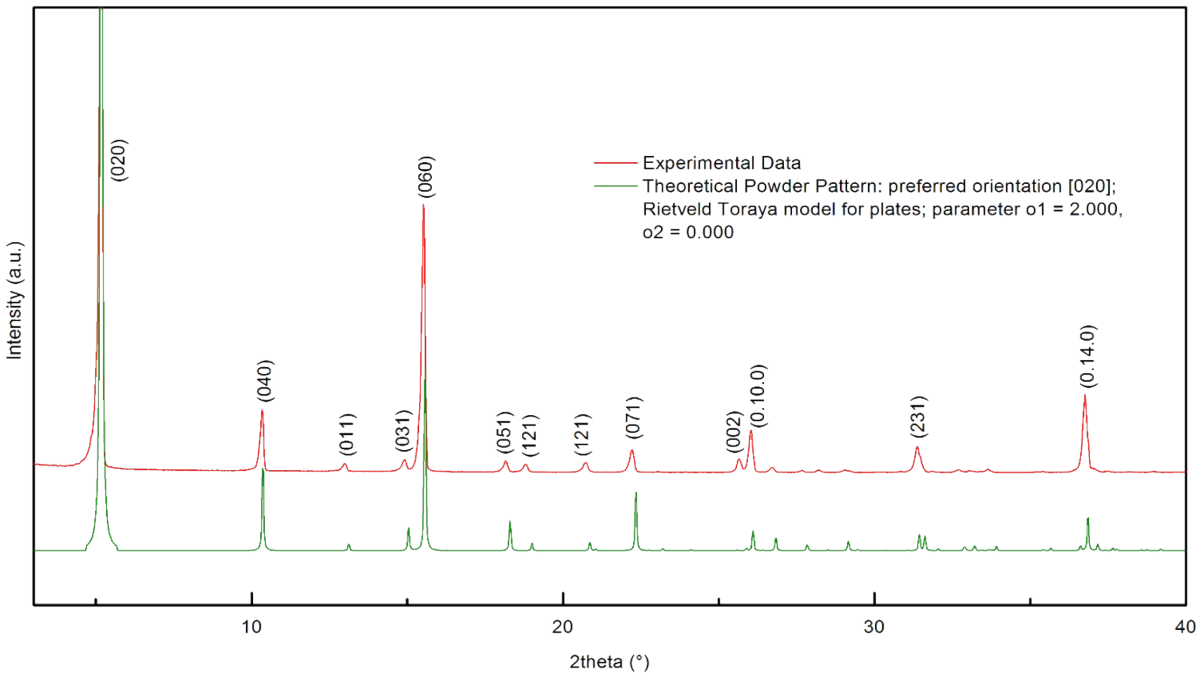

Figure S1. Powder diffractograms for **1**.

X-ray structure determination

Single-crystal X-ray data of sample was collected on a Oxford Diffraction Xcalibur diffractometer equipped with a Sapphire3 CCD detector and a graphite monochromator utilizing MoKα radiation (λ = 0.71073 Å). Empirical absorption corrections were based on the multi-scan technique using spherical harmonics, implemented in SCALE3 ABSPACK scaling algorithm.[2] The minimum and maximum transmission factors were T_{min} = 0.7597, T_{max} = 1.0000. The structures were solved by SHELXT-2015[3] and refined against the F^2 data using full-matrix least squares methods with the program SHELXL-2014/7.[4] Anisotropic displacement parameters were refined for all non-H atoms. The positional parameters of the hydrogen atoms bonded to carbon and oxygen atoms were refined with isotropic displacement parameters assigned as 1.2 times the U_{eq} values of the corresponding bonding partners. The structural figures were drawn using Diamond.[5]

Crystallographic data for the compound **1** (CCDC 1536321) has been deposited with the Cambridge Crystallographic Data Centre. These can be obtained free of charge from The Cambridge Crystallographic Data Centre via www.ccdc.cam.ac.uk/data_request/cif.

References

1. Kraus, W. & Nolze, G. J. Appl. Cryst. 1996, 29, 301–303.
2. Oxford Diffraction 2006 CrysAlisPro CCD and CrysAlisPro RED.
3. SHELDRICK, George M. SHELXT – Integrated space-group and crystal-structure determination. Acta Crystallogr. 2015, A71(1), 3-8.
4. Sheldrick, G. M. Acta Cryst. 2008 A64, 112.
5. Brandenburg, K.; Putz, H. DIAMOND. Crystal Impact GbR 1999 Bonn, Germany.

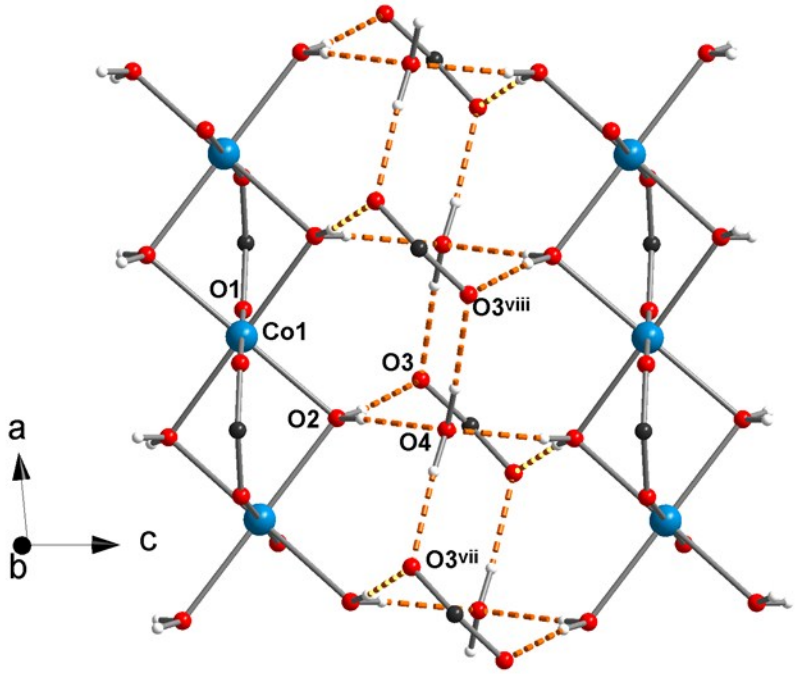

Figure S2 View of the hydrogen bonding system in **1** approximatively along the *b* axis linking the chains. Aromatic rings are omitted for clarity. The O···O distances are from the range 2.630(2)-2.681(2) Å. Symmetry codes: vii: x-0.5, -y+1, z; viii: 1-x, 1-y, 1-z.

Table S1. Possible hydrogen bonds (Å, º) for **1.**

D-H···A	*d(D-H)*	*d(H···A)*	*d(D···A)*	*<(DHA)*
O2-H2A···O3	0.85(3)	1.79(3)	2.630(2)	170(3)
O2-H2B···O4	0.77(3)	1.93(3)	2.679(2)	163(3)
O4-H4A···O3^{vii}	0.85(3)	1.84(3)	2.681(2)	175(3)

Symmetry code: vii: x-0.5, -y+1, z.

AC susceptibility data

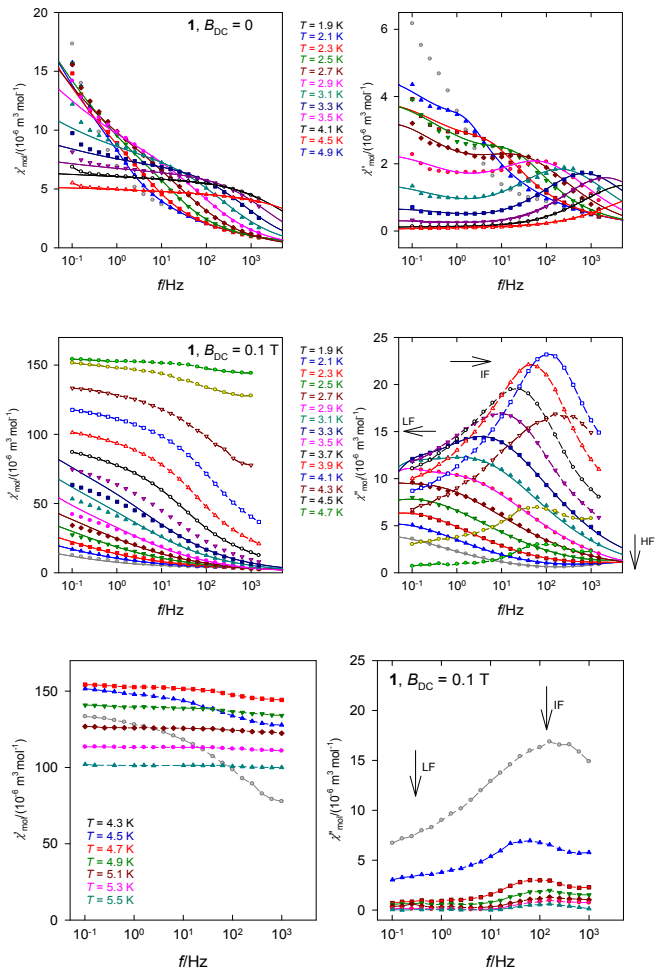

Frequency dependence of the AC susceptibility components

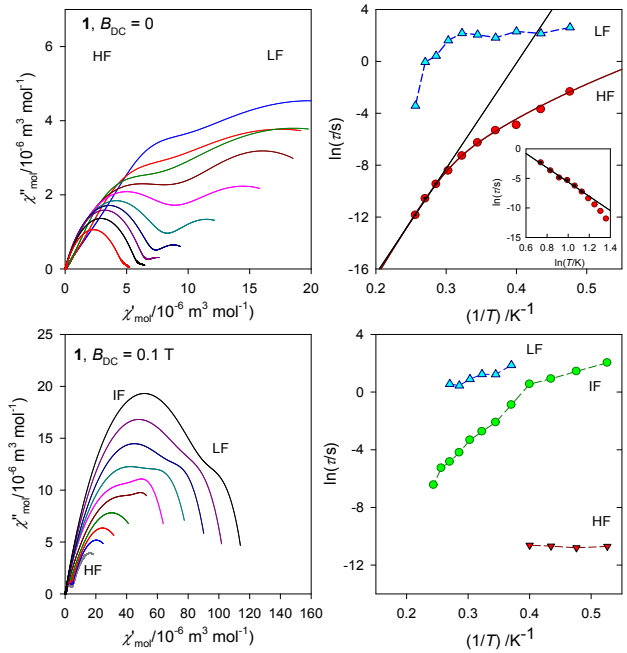

Argand and Arrhenius-like plots

Figure S3. AC susceptibility data for **1** at different DC magnetic field and varied temperature.

Table S2. Results of the fitting procedure for AC susceptibility components of **1.**

a) at B_{DC} = 0 with a two-set Debye model; χ_S = 0

T/K	$R(\chi')$ /%	$R(\chi'')$ /%	χ_{T1}	α_1	τ_1 / s	χ_{T2}	α_2	τ_2 / 10^{-3} s	x_{LF}
2.1	7.1	3.4	37(14)	0.69(5)	14(35)	38(16)	0	95(39)	0.97
2.3	4.1	4.8	31(10)	0.70(4)	8.5(215)	33(11)	0.19(26)	25(10)	0.94
2.5	4.5	5.0	31(8)	0.70(2)	10(18)	34(8)	0.26(16)	7.3(25)	0.91
2.7	5.7	4.2	17(30)	0.56(50)	6.2(268)	25(24)	0.48(10)	4.8(48)	0.68
2.9	5.6	4.6	14(36)	0.62(62)	7.8(586)	22(29)	0.46(18)	1.8(14)	0.64
3.1	6.9	3.9	8.0(243)	0.60(66)	8.7(916)	16(21)	0.46(8)	0.69(35)	0.50
3.3	4.9	2.6	4.0(92)	0.61(53)	5.0(412)	11(8)	0.43(6)	0.22(5)	0.36
3.5	3.9	2.4	1.5(28)	0.58(56)	1.5(82)	7.9(23)	0.42(6)	0.077(13)	0.19
3.7	2.7	2.9	0.95(329)	0.69(90)	0.94(921)	6.7(23)	0.44(10)	0.025(4)	0.14
3.9	2.2	6.5	0.78(203)	0.7(6)	0.03(26)	5.3(5)	0.45(22)	0.0071(23)	0.15

b) at B_{DC} = 0.1 with a two-set Debye model; χ_S = 0

T/K	$R(\chi')$ /%	$R(\chi'')$ /%	χ_{T1}	α_1	τ_1 / s	χ_{T2}	α_2	τ_2 / s	χ_{T3}	α_3	τ_3 / 10^{-6}s
1.9	5.7	1.9	-	-	-	25(9)	0.61(6)	7.6(114)	28(9)	0.31(27)	22(12)
2.1	3.9	1.2	-	-	-	34(7)	0.62(4)	4.2(33)	37(6)	0.39(27)	20(11)
2.3	3.7	1.0	-	-	-	43(7)	0.63(4)	2.5(15)	46(6)	0.41(29)	23(17)
2.5	5.2	1.5	-	-	-	58(9)	0.66(4)	1.7(12)	59(8)	0.06(162)	25(65)
2.7	7.2	1.6	9	0	16	73.7	0.65	0.59	74.0	0.10	21
2.7	6.6	1.1	7(76)	0.01(265)	6.4(770)	67(59)	0.65(3)	0.41(71)			
2.9	9.4	0.74	10(54)	0.14(173)	3.3(154)	72(29)	0.61(5)	0.12(24)			
3.1	12.3	1.4	13(75)	0.22(186)	3.4(192)	86(43)	0.61(5)	0.064(128)			
3.3	12.7	0.8	11(69)	0.16(221)	2.4(132)	97(40)	0.59(6)	0.036(59)			
3.5	12.7	1.7	16(70)	0.26(170)	1.6(54)	106(35)	0.56(7)	0.015(23)			
3.7	10.4	1.8	18(59)	0.26(137)	1.7(62)	118(38)	0.54(5)	0.0079(70)			
3.9	8.7	1.8	24(63)	0.37(107)	1.3(42)	129(40)	0.51(6)	0.0033(25)			
4.1	10.2	2.2	34(186)	0.55(182)	1.2(89)	142(111)	0.51(12)	0.0012(17)			